Electron-impact excitation of the resonance transition in Be^+

J. Mitroy and D. W. Norcross*
Joint Institute for Laboratory Astrophysics, University of Colorado and National Bureau of Standards, P.O. Box 440, Boulder, Colorado 80309-0440
(Received 14 October 1987)

The cross section for electron-impact excitation of the resonance transition ($2s$-$2p$) of Be^+ has been calculated in a variety of models at low incident-electron energies. Both five-state ($2s,2p,3s,3p,3d$) and nine-state ($2s-3d,\overline{4s},\overline{4p},\overline{4d},\overline{4f}$) close-coupling (with and without polarization potentials) calculations have been completed. The results, while in good agreement with previous calculations, do not resolve all the long-standing discrepancies between theory and experiment. There are still significant discrepancies with the experimental cross section for the $2s$-$2p$ transition. However, previous calculations of the polarization of the resonance fluorescence used an expression for the scattering amplitude that was inappropriate for ions. The present results for the polarization use the correct expression, and are in good agreement with experiment. Calculations using the same approach for other quantities, specifically binding energies and resonance parameters, show small but significant improvements when compared with experiment.

I. INTRODUCTION

This paper is an attempt to resolve the long-standing problems with regard to the electron-impact excitation of the resonance transition ($2s$-$2p$) of Be^+. Notable discrepancies, at the order of 15–20% exist between theoretical predictions[1–3] and experimental data[4] for this transition. At energies just above the $2p$ excitation threshold, the calculated cross sections exceed the measurements by about 20%, which is substantially larger than the quoted high-confidence level (98%) uncertainty of about 10% attributed to the data. The calculated linear polarization of the fluorescence radiation for this doublet also shows serious discrepancies when compared with experiment, especially near threshold where it exceeds the experimental data by about 50%. From the theoretical point of view these discrepancies are extremely serious. The Be^+ system is a relatively simple ion, so we would intuitively expect that calculations should be able to reproduce the experimental cross sections to quite high accuracy. Failure to reproduce the experimental data for this simple system must raise questions about the accuracy of calculations on more complicated ionic systems, so it is clear that the issue should be resolved.

The Be^+ system consists of a weakly bound valence electron ($\varepsilon_{2s} \sim 0.7$ a.u.) located outside a tightly-bound ($\varepsilon_{1s} \sim 6$ a.u.) heliumlike core. As a consequence the earliest close-coupling (CC) calculations[1,2] used target wave functions in which the core was assumed to be inert and only the valence electron could be excited. The first of these calculations[1] was done in both the two-state ($2s,2p$) and five-state ($2s,2p,3s,3p,3d$) approximations. In that calculation, the effects of including semiempirical core polarization potentials for both the valence and scattered electrons were also investigated. There was improvement (i.e., a decrease in the cross section) in going from the two-state to the five-state approximation. The other calculation[2] also had five states explicitly coupled in the CC expansion. However, the $n=3$ levels were represented by pseudostates which were chosen to minimize the partial cross sections for the dominant partial waves. There was reasonable agreement between these two different five-state calculations, although the pseudostate calculation reported slightly smaller cross sections, in somewhat better agreement with experiment. However, the drop in the cross section was not nearly enough to rationalize the differences between theory and experiment.

The most recent attempt[3] to resolve the problem investigated whether the processes inducing the transition of the valence electron could be influenced by the details of valence-core electron correlations. While this calculation was also done at the five-state level, the target states were approximated by quite complicated configuration interaction wave functions,[3] whereas previously[1,2] the target wave functions used were single-configuration wave functions. There were no significant improvements in the predicted cross sections in this calculation.[3]

In the present work, we have decided to investigate the possible influence of using a very extensive set of target states (five physical and four pseudostates) on the cross section for the $2s$-$2p$ transition. The reasons for this calculation are several. First, while the calculations using a pseudostate basis[2] did yield smaller total cross sections than the calculations using wave functions approximating only the physical states, they were carried out at energies above the ionization threshold, and thus the size of the effect for energies close to threshold remained unknown. It is known, for instance, that at energies above the ionization threshold the ionization cross section[5] is a significant fraction ($\sim 10\%$) of the $2s$-$2p$ cross section. Since pseudostates can be interpreted as a mechanism for incorporating virtual transitions (our pseudostate calculations are restricted to a maximum incident energy of 0.5 a.u.) into the ionization continuum, these additional

long-range correlations are incorporated in our calculations. Finally, an exhaustive calculation, if undertaken in a systematic fashion, should give not only a more accurate cross section, but also some indication of how close the calculation is to convergence with respect to the inclusion of additional states in the CC expansion. The results of the present calculation indicate that the addition of the four pseudostates does *not* change the calculated excitation cross sections by enough to significantly reduce the discrepancy between the calculated and measured cross sections.

Discrepancies between theory[1,3] and experiment[4] were also found for the polarization of the resonance fluorescence of the $2p$ state. However, it has since been learned[6] that the earlier calculations of the polarization of the fluorescence radiation were incorrect due to the use of an expression[7] for the scattering amplitude that was inappropriate for ions. The present results, which use the correct expression, agree with the experimental data.

The details of the target physical states and pseudostates are described in Sec. II. In this section we also describe the different types of calculations we have done. Section III contains the results of calculations undertaken on the binding energies of the Be atom. In Sec. IV the results of calculations giving details of resonance positions and widths of the $Be^+ + e^-$ system are reported. Section V contains the results of cross-section calculations for the $2s$-$2p$ transition. Cross sections for electron-impact excitation of the $3s$, $3p$, and $3d$ levels are also given. Section VI contains the calculated fluorescence polarizations for the $2p$-$2s$ decay which now agree with experiment. In Sec. VII the variation of a few selected properties (BeI binding energies, partial cross sections) with the specific choice of the pseudostate is studied. In Sec. VIII the work is summarized and its significance discussed.

II. DETAILS OF THE CALCULATIONS

Since previous calculations[1,3] have demonstrated that multiconfiguration and single-configuration descriptions of the target states give very similar results, we have adopted a single-configuration representation for the target states. The wave functions used in this study were computed using an analytic Hartree-Fock (HF) program written by one of us (J.M.). These wave functions were processed and then fed into the COLALG[8] and IMPACT[9] suite of programs.

The program IMPACT sets up and solves a set of linear algebraic equations.[10] The radial mesh used for the present calculations was more dense (e.g., 80 points) than would normally be the case for an IMPACT calculation on such a light system. We wanted to be certain that the details of the numerical analysis would have no effect on the computed cross section. IMPACT uses the usual (real) asymptotic form of the wave function

$$F_{ij}(r) \sim k_i^{-1/2}(\delta_{ij}\sin\theta_i + K_{ij}\cos\theta_i) \quad \text{as } r \to \infty \ , \tag{1}$$

where

$$\theta_i = k_i r - \tfrac{1}{2} l_i \pi + \frac{z}{k_i}\ln(2k_i r) + \sigma_{l_i} \ , \tag{2}$$

z is the asymptotic charge, and σ_{l_i} is the Coulomb phase shift. With these definitions the scattering amplitude for an inelastic transition between states i and j with quantum numbers L_i, M_{L_i}, S_i, and M_{S_i}, and L_j, M_{L_j}, S_j, and M_{S_j} is (for an electron beam incident in the $\hat{z}$ direction)

$$f_{ij} = -i(\pi/k_i k_j)^{1/2} \sum_{\substack{L,S,\pi \\ l_j,l_i,m_j}} i^{l_i - l_j} e^{i(\sigma_{l_i}+\sigma_{l_j})}(2l_i+1)^{1/2} \times (S_i M_{S_i} \tfrac{1}{2}\mu_i \mid SM_S)(L_i M_{L_i} l_i 0 \mid LM)(S_j M_{S_j} \tfrac{1}{2}\mu_j \mid SM_S)(L_j M_{L_j} l_j m_j \mid LM) T_{l_i l_j}^{LS\pi} Y_{l_j m_j}(\hat{k}_j) \ , \tag{3}$$

where the $\underline{T}$ matrix is defined by

$$\underline{T} = \underline{1} - \underline{S} \quad \text{and} \quad \underline{S} = (\underline{1} + i\underline{K})(\underline{1} - i\underline{K})^{-1} \ . \tag{4}$$

The total inelastic cross section obtained by averaging (summing) over initial (final) angular momentum and spin states and integrating over angles does not contain an explicit reference to the Coulomb phase. The total inelastic cross section is

$$Q(i \to j) = \frac{\pi}{k_i^2} \sum_{\substack{L,S,\pi \\ l_i,l_j}} \frac{(2L+1)(2S+1)}{2(2L_i+1)(2S_i+1)} \mid T_{l_i l_j}^{LS\pi} \mid^2 \ . \tag{5}$$

However, the Coulomb phase must be retained when anything other than the total cross section is calculated. An example of this occurs in the calculation of excitation cross sections for the different magnetic substates. When the spin variables are averaged and angular integrations performed, the partial cross section becomes

$$Q(i \to j, M_{L_j}) = \frac{\pi}{k_i^2} \frac{1}{2(2S_i+1)(2L_i+1)} \sum_{S,\pi,M_{L_i},l_j,m_j} (2S+1) \times \left| \sum_{L,l_i} (2l_i+1)^{1/2} i^{l_i} e^{i\sigma_{l_i}} (L_i M_{L_i} l_i 0 \mid LM)(L_j M_{L_j} l_j m_j \mid LM) T_{l_i l_j}^{LS\pi} \right|^2 \ . \tag{6}$$

This equation differs from that of Saraph[7] [Eq. (3.3)] by precisely the Coulomb phase associated with scattering from the *initial* state. Previous calculations[1,3] of these partial cross sections, which are needed for the calculation of the polarization of the fluorescence radiation of the $2p$ state, used the incorrect expression and are in error.[6]

The simplest calculation was at the five-state $(2s,2p,3s,3p,3d)$ level of approximation. A very extensive Slater-type-orbital (STO) basis was used in the computation of the Hartree-Fock (HF) wave functions. The basis set used by Weiss[11] was augmented by extra STO's in order to improve the quality of the wave functions. Comparison of HF energies for the Be^+ $1s^2 2p$ state gives an idea of the completeness of our STO basis. The energy obtained using the numerical (multiconfiguration Hartree-Fock) MCHF77[12] program is $-14.130\,860$ a.u.; the HF energy obtained using the present STO basis is $-14.130\,858$ a.u. The valence wave functions for the $(2s,2p,3s,3p,3d)$ states were computed in the frozen-core approximation. The $(1s)^2$ core was obtained from a calculation of the Be^+ $1s^2 2p$ state. The calculated and experimental[13] (averaged for spin-orbit splitting) binding energies for the Be^+ system are shown in Table I. There are discrepancies between the HF binding energies and experiment, but they are less than 1%. Calculations using this set of HF target states will be referred to in future as CC5.

Although the HF binding energies (and consequently excitation energies) are in good accord with experiment, the small errors in the excitation energies enter the calculation of the cross section in a fairly direct manner and should be corrected if possible. This can be done by using a semiempirical polarization potential to incorporate the effects of core-valence electron correlations. The polarization potential used is due to Norcross and Seaton,[14] and is

$$V_p = -\frac{\alpha_d}{2r^4}[1-\exp(-r^6/\rho_l^6)] \ . \tag{7}$$

In the above expression α_d is the value of the dipole polarizability of the Be^{++} $(1s)^2$ core, and the parameters ρ_l were fixed empirically. The polarization potential was added to the HF Hamiltonian for the valence electron, and the valence orbitals recomputed. The specifications of the Be^{2+} $1s^2$ core were fixed at those for the calculations without the polarization potential. The value used for the dipole polarizability[15] α_d is 0.0522 a.u. The parameters ρ_l were determined by fitting the calculated binding energies for the Be^+ $l=0$, 1, and 2 states to the experimental energies. Values of 0.9616, 0.9074, and 1.326 a.u. were obtained for ρ_0, ρ_1, and ρ_2, respectively. We took $\rho_l = 1.326$ for $l > 2$. Values of the binding energies for the $2s$, $2p$, $3s$, $3p$, and $3d$ states computed with these values of the polarization parameters are also given in Table I. The differences between theory and experiment were reduced to less than 10^{-4} a.u. in all cases.

TABLE I. Binding energies (in a.u.) for the five lowest states of the Be^+ system for different models compared. The binding energies in the fixed core HF approximation are in the column labeled CC5 and those computed with an additional polarization potential are in the column labeled CC5V. The energy of the $1s^2$ core is the same for both calculations and is $-13.611\,14$ a.u.

State	CC5	CC5V	Expt.
$2s$	$-0.666\,222$	$-0.669\,247$	$-0.669\,244$
$2p$	$-0.519\,714$	$-0.523\,787$	$-0.523\,746$
$3s$	$-0.266\,525$	$-0.267\,186$	$-0.267\,230$
$3p$	$-0.228\,496$	$-0.229\,534$	$-0.299\,573$
$3d$	$-0.222\,296$	$-0.222\,474$	$-0.222\,473$

Since polarization potentials have been introduced to improve the quality of the wave functions for the valence electron, it is necessary from considerations of consistency to allow for the influence of polarization potentials on the second "scattered" electron. Furthermore, it has been shown that a dielectronic polarization potential should also be included.[14] We used the form

$$V_{\text{diel}} = -\frac{\alpha_d \hat{r}_1 \cdot \hat{r}_2}{r_1^2 r_2^2}\left\{\left[1-\exp\left[-\frac{r_1^6}{\bar{\rho}^6}\right]\right] \times \left[1-\exp\left[-\frac{r_2^6}{\bar{\rho}^6}\right]\right]\right\}^{1/2} , \tag{8}$$

where α_d is the dipole polarizability and $\bar{\rho}$ was chosen to be 0.98 a.u. This value was chosen by taking a weighted average of ρ_0, ρ_1, and ρ_2 biased towards the lower partial waves. The calculation that used polarization potentials for both the target and scattering electron, including the dielectronic term, will be referred to henceforth as the CC5V model.

In order to allow for the effect of virtual transitions to the continuum we also performed a calculation in which the five states of the CC5V expansion were supplemented by a set of four, $n=4$ (i.e., $\overline{4s},\overline{4p},\overline{4d},\overline{4f}$) pseudostates. The prescription for the calculation for these states was as follows: the pseudostates were chosen to have the initial form

$$\bar{\Psi}_{nl}(r) = 0.1\left[\frac{\left[\frac{2Z}{l+1}\right]^{2l+1}}{(2l)!}\right]^{1/2} r^{l-1}e^{-Zr/l+1} + 0.9\left[\frac{(2\alpha_l)^{2l+5}}{(2l+4)!}\right]^{1/2} r^{l+1}e^{-\alpha_l r} , \tag{9}$$

where Z is the nuclear charge. These states were then orthogonalized with respect to the low-lying $n=2$ and $n=3$ "physical" orbitals. The energies of these states were then evaluated (the polarization potential was included for this) and the parameter α_l adjusted until the energies of the four pseudostates were degenerate to some specified tolerance (e.g., 10^{-5} a.u.). The pseudostate excitation energies were chosen to be degenerate to facilitate the solution of the CC equations in IMPACT. The excitation energy from the $2s$ ground state then becomes a convenient parameter with which to characterize the pseudostate basis. Because of the problem of pseudoresonances occurring near the excitation energies of the pseudo-

TABLE II. Oscillator strengths for various transitions for the Be^+ ion. The columns labeled PNP are from Parpia, Norcross, and da Paixao (Ref. 3) and those labeled CC5 and CC5V were obtained using wave functions described in the text. The energy differences used in calculating the oscillator strengths came from the theory.

	CC5		CC5V		PNP	
Transition	f_l	f_v	f_l	f_v	f_l	f_v
$2s$-$2p$	0.5142	0.5468	0.5045	0.5391	0.5051	0.4938
$2s$-$3p$	0.0780	0.0812	0.0771	0.0816	0.0793	0.0812
$2p$-$3s$	0.0654	0.0644	0.0638	0.0666	0.0649	0.0644
$2p$-$3d$	0.6424	0.6320	0.6349	0.6327	0.6327	0.6320

states, solutions for this model were only obtained for $E \leq 0.5$ a.u. It will be seen in Sec. VII that the results of the calculations are relatively insensitive to the particular choice of the pseudostate excitation threshold. For the results of calculations presented in Secs. III–IV a value of $\bar{\varepsilon}=0.9$ a.u. was used for the pseudostate threshold. The corresponding values of α_l are 1.247 26, 1.502 07, 2.392 88, and 2.022 27 for $l=0$, 1, 2, and 3, respectively. These calculations will be designated CC9V.

In Table II we compare oscillator strengths computed with the CC5 and CC5V wave functions to get some idea of the differences in the two sets of wave functions. We did not include a core-polarization correction to the dipole length operator when calculating the oscillator strength in the length gauge. The small size of the dipole polarizability would cause any correction to be small, e.g., including a core-polarization correction changes the dipole length matrix element by less than 1%. Agreement between length (f_l) and velocity (f_v) gauges is a necessary, although not sufficient, condition that the exact wave function must satisfy. The calculations of Parpia, Norcross, and da Paixao[3] (referred to as PNP) give smaller differences between f_l and f_v than the present single-configuration calculations. The CC5 and CC5V calculations generally give values for f_l and f_v that are roughly the same. However, for the transition in which we are specifically interested, namely, the $2s$-$2p$ transition, the CC5V f_l is closer to the PNP f_l than is the CC5 f_l. We did not include any experimental f values in Table II since these are not sufficiently precise[3] to discriminate between the different values for the oscillator strengths.

III. CALCULATION OF Be BINDING ENERGIES

While our ultimate goal is the computation of the cross section and fluorescence polarization for the Be^+ $2s$-$2p$ transition, a good test of the accuracy of our models for the $Be^+ + e^-$ system lies in the calculation of Be atomic binding energies. To do this requires the calculation of the $Be^+ + e^-$ system wave functions with a decaying exponential (instead of sinusoidal) boundary condition for the "scattering" electron. Calculations of the Be atom binding energies have been carried out by a number of authors.[3,14,16,17] We include only the results of the most modern[3,16] calculations along with the present work in Table III, since these calculations and the present calculations supersede some of the older[14,17] results.

The comparison of the HF binding energies with the CC values shows the importance of including long-range correlations in the wave functions. Comparison of the CC5 and CC5V energies shows that the polarization po-

TABLE III. Binding energies (in a.u.) of Be atom states relative to the series limit (the Be^+ $2s$ state) at 0.342 60 a.u.

State	HF	PNP[a]	MS[b]	CC5	CC5V	CC9V	Expt.[c]
$2s^2\,{}^1S^e$	−0.295 64	−0.342 03	−0.341 53	−0.340 97	−0.341 93	−0.342 52	−0.342 60
$2s3s\,{}^1S^e$	−0.097 84	−0.093 38	−0.093 11	−0.093 28	−0.093 36	−0.093 48	−0.093 47
$2s3s\,{}^3S^e$	−0.100 10	−0.105 29	−0.104 81	−0.105 07	−0.105 26	−0.105 29	−0.105 30
$2s2p\,{}^1P^o$	−0.117 35	−0.146 30	−0.147 57	−0.145 30	−0.146 70	−0.148 21	−0.148 66
$2s3p\,{}^1P^o$	−0.555 95	−0.067 71	−0.067 93	−0.067 35	−0.067 81	−0.068 22	−0.068 37
$2s2p\,{}^3P^o$	−0.234 13	−0.241 36	−0.241 38	−0.240 96	−0.242 12	−0.242 48	−0.242 45
$2s3p\,{}^3P^o$	−0.071 47	−0.074 11	−0.073 91	−0.073 94	−0.074 10	−0.074 16	−0.074 20
$2p^2\,{}^3P^e$	−0.058 92	−0.067 11	−0.069 80	−0.066 54	−0.068 83	−0.070 43	−0.070 61
$2p^2\,{}^1D^e$	−0.025 42	−0.081 66	−0.082 47	−0.081 97	−0.082 72	−0.083 35	−0.083 43
$2s3d\,{}^1D^e$	−0.055 17	−0.048 38	−0.048 38	−0.048 34	−0.048 71	−0.048 94	−0.049 04
$2s3d\,{}^3D^e$	−0.056 74	−0.059 76	−0.059 63	−0.059 85	−0.059 82	−0.059 86	−0.059 86
$2s4f\,{}^1F^o$	−0.031 24	−0.031 67		−0.031 67	−0.031 67	−0.031 67	−0.031 67
$2s4f\,{}^3F^o$	−0.031 26	−0.031 67		−0.031 67	−0.031 67	−0.031 67	−0.031 67

[a]Reference 3.
[b]Reference 16.
[c]Reference 13.

TABLE IV. Resonance positions (ε) and widths (Γ) (in a.u.) for some of the Be resonances below the Be^+ $2p$ excitation threshold.

	Expt.		NS[b]		MS[c]		CC9V	
Resonance	ε	Γ[a]	ε	Γ	ε	Γ	ε	Γ
$2p^2\,{}^1S^e$	0.004 54[d]	3.4[−4]	0.0121	3.86[−4]	0.006 97	3.30[−4]	0.005 86	3.40[−4]
$2p3p\,{}^1S^e$					0.091 67	3.14[−4]	0.0904	3.02[−4]
$2p3p\,{}^3S^e$	0.0742[e]		0.0748	3.78[−4]	0.075 62	4.24[−4]	0.0741	4.27[−4]
$2p3s\,{}^1P^o$			0.0604	1.84[−2]			0.0588	1.78[−2]
$2p3d\,{}^1P^o$	0.0933[f]				0.095 68	4.04[−6]	0.0933	1.74[−5]
	0.093 32[d]							
$2p3s\,{}^3P^o$	0.0473[g]	<7.2[−6]	0.0482	1.09[−5]	0.048 46	5.16[−6]	0.0472	8.53[−7]
$2p3d\,{}^3P^o$					0.093 52	4.70[−4]	0.0912	4.70[−4]
$2p3p\,{}^1D^e$			0.0785	4.10[−3]	0.079 13	4.00[−3]	0.0778	3.77[−3]
$2p3p\,{}^3D^e$			0.0681	7.60[−5]	0.069 05	3.22[−5]	0.0672	5.50[−5]
$2p3d\,{}^1F^o$			0.0928	3.28[−3]			0.0921	3.18[−3]
$2p3d\,{}^3F^o$			0.0861	5.60[−3]			0.0854	5.04[−3]

[a]The notation $a\,[-b]$ means $a\times10^{-b}$.
[b]Reference 14.
[c]Reference 16.
[d]Reference 18.
[e]Reference 19.
[f]Reference 20.
[g]References 21 and 22.

tential makes a small ($\sim10^{-3}$ a.u.) but important correction to the predicted binding energies. Further evidence for the importance of the core-valence polarization potential is provided by the comparison of the CC9V results with those of Moccia and Spizzo[16] (MS). The calculation by MS was a quite extensive *ab initio* calculation, but with correlations between only the two valence electrons taken into consideration. The CC9V calculation was at a similar level of accuracy for the outer shell, but core-valence correlations were also included semiempirically. The theoretical predictions of the CC9V model are, in every case, in better accord with experiment. The *largest* discrepancy with experiment (for the CC9V model) occurs for the $2s2p\,{}^1P^o$ state and is only 4.5×10^{-4} a.u. (i.e., 0.015 eV). By contrast, the MS calculations (and all the other models) give energies which have much larger differences ($>10^{-3}$ a.u.) with experiment.

These results indicate that if the binding energies of the Be atom are to be predicted with the highest accuracy, it is necessary to allow for core-valence correlations as well as to have a large basis in which to expand the valence two-electron wave function.

IV. RESONANCE POSITIONS AND WIDTHS

While the calculation of the Be atom binding energies indicates that we have a good model of the $Be^+ + e^-$ system, further confirmation can be obtained by comparing calculated resonance positions and widths with experimental data. The positions and widths of a number of resonances (in the elastic scattering region) have been detailed in Table IV. Since the determination of the resonance parameters is quite time consuming, and the experimental data rather scarce, we have not presented values for a series of increasingly bigger calculations, but rather values for only the CC9V calculation. The resonance parameters were determined by fitting the phase shifts to the formula

$$\delta=\delta_0+b(E-\varepsilon_0)+\arctan\left[\frac{\Gamma}{2(\varepsilon_0-E)}\right]+\pi\theta(E-\varepsilon_0)\ , \tag{10}$$

where θ is the Heaviside function. In the above equation ε_0 is the resonance position and Γ is the width (full width half-maximum). It is apparent in all cases that the CC9V model predicts resonance positions lower in energy than the other models. In those instances where experimental data exists, the CC9V calculations are in better agreement with experiment.

Particular attention is focused upon the $(2p)^2\,{}^1S^e$ resonance in Table V, since this is the only resonance for

TABLE V. Positions and widths (in a.u.) of the $2p^2\,{}^1S^e$ resonance. The first column gives the number of states included in the CC expansion. The column labeled ε gives the resonance position relative to the $Be^+\,{}^2S^e$ state and that labeled Γ the full width at half-maximum.

Number of states	Determination	ε	Γ[a]
2 ($2s,2p$)	PNP[b]	0.0294	8.23[−6]
3 ($2s,2p,3s$)	PNP	0.0288	3.9[−8]
($2s,2p,\overline{3d}$)	NS[c]	0.0121	3.86[−4]
4 ($2s,2p,3s,3p$)	PNP	0.0282	5.20[−6]
5 ($2s,2p,3s,3p,3d$)	PNP	0.0124	2.44[−4]
	CC5	0.0127	2.47[−4]
	CC5V	0.0111	2.69[−4]
Not relevant	MS[d]	0.006 97	3.30[−4]
9 ($2s,2p,3s,3p,3d,$ $\overline{4s},\overline{4p},\overline{4d},\overline{4f}$)	CC9V	0.005 86	3.40[−4]
	Expt.[e]	0.004 54	3.4[−4]

[a]The notation $a\,[-b]$ means $a\times10^{-b}$.
[b]Reference 3.
[c]Reference 14.
[d]Reference 16.
[e]Reference 18.

TABLE VI. Partial-wave contributions to the $2s$-$2p$ cross section (in units of πa_0^2) for Be^+ near threshold ($E=0.15$ a.u.). The results of three five-state calculations and one nine-state calculation are presented.

L	PNP[a]	CC5	CC5V	CC9V
0	0.258	0.258	0.266	0.283
1	2.878	2.914	2.897	2.854
2	1.535	1.590	1.514	1.384
3	10.895	11.008	10.918	10.745
4	5.079	5.233	5.260	5.218
5	1.089	1.142	1.181	1.175
6	0.158	0.170	0.183	0.182
7	0.017	0.019	0.021	0.021
8	0.001	0.002	0.002	0.002
9 and up	$<2\times10^{-4}$	$<2\times10^{-4}$	$<2\times10^{-4}$	$<2\times10^{-4}$
Total	21.91	22.34	22.24	21.86

[a]Reference 3.

which a reliable value for the width[18] is available. While there is a 20% error in the CC9V prediction of the resonance position, the absolute error is only 0.0012 a.u. (i.e., $\frac{1}{20}$ eV), which could easily be due to the slow convergence of the CC expansion for this particular resonance. However, the value predicted for the width is in very good accord with the experiment.

V. CROSS-SECTION RESULTS

The linear-algebraic method embodied in the IMPACT code was used to solve the close coupling equations for partial waves from $L=0$ to $L=10$. The partial-wave sum was completed using five-state unitarized Coulomb-Born results. A detailed comparison of the partial-wave cross sections near threshold is shown in Table VI. We compare results from the present work with those of Parpia, Norcross, and da Paixao.[3] The five-state results of Hayes *et al.*[1] are not tabulated as the particular choice of the numerical grid parameters were not as stringent as those used in the more recent calculations.

The largest variations in the individual partial cross sections occur for the $^1S^e$ and $^1D^e$ symmetries. This is to be expected since configuration interaction effects caused by the $2p^2\,^1S^e$ and $2p^2\,^1D^e$ perturbers are known to be very strong for the $^1S^e$ and $^1D^e$ bound states of the Be atom (see Table III). The variations in partial cross sections for the other partial waves is much smaller. For instance, there is only a variation of about 2–3% in the cross section for the $L=1$, 3, and 4 waves. This is significant since these are the partial waves which make up more than 80% of the total cross section at threshold.

The variations in the partial cross sections of the different models for $L\geq5$ is probably a kinematic effect. The PNP, CC5, and CC5V models all used wave functions with the $2p$ excitation threshold located at different energies. Since the partial cross sections for the higher L values increase rapidly near threshold as the energy of the outgoing electron (after $2p$ excitation) is increased, the differences in the partial cross sections for high L are probably due to the different $2s$-$2p$ excitation energies for the different calculations.

Total cross sections for the Be^+ $2s$-$2p$ transition are presented in Table VII. The influence of a number of partially resolved resonances associated with the closed $n=3$ channels can be seen as irregularities in the cross sections for incident energies between 0.3 and 0.4 a.u. Since the fluctuations in the cross section are only of the order of 5%, a meaningful comparison with experiment is possible without a complete analysis of the resonance structure. Comparison of the CC5 and CC5V calculation shows that inclusion of the polarization potential generally results in a small decrease ($\sim1\%$) in the total cross section. The inclusion of the $n=4$ pseudostates also leads to a small decrease (~1–2%) in the cross section. This is clearly seen by comparing the CC5V and CC9V results. The comparison with the experimental data is presented in graphical form in Fig. 1. The results of our best calculation are larger than the experimental data by about 20% at all energies.

In Table VIII we present partial cross sections for exciting the $2p$ $M=0$ and $M=1$ magnetic substates. The values of PNP are not presented since they used an expression for the partial cross section which is incorrect for ions.[6] The differences between the different calculations are generally less than 5% except for incident energies between 0.3 and 0.4 a.u. where the resonance structure complicates the situation.

For completeness we also tabulate total cross sections for excitation to the $3s$, $3p$, and $3d$ states in Table IX. The CC9V results are some 10–20% smaller than the five-state calculations. This is an indication that coupling between the $n=3$ and higher levels is important if

TABLE VII. The total cross sections (in units of πa_0^2) for excitation from the $2s$ level to the $2p$ level as a function of incident energy (in a.u.). The results of four different calculations are presented.

Energy	PNP[a]	CC5	CC5V	CC9V
0.15	21.9	22.33	22.24	21.86
0.175		20.91	20.82	20.44
0.20	19.4	19.81	19.70	19.34
0.225		18.90	18.78	18.42
0.250	17.8	18.15	18.02	17.70
0.275		17.85	17.55	17.21
0.300	16.0	17.15	16.42	16.18
0.325		16.33	16.29	15.99
0.350	15.5	14.90	15.85	15.51
0.375		15.68	14.99	14.77
0.400	14.7	14.74	14.70	14.40
0.450	13.2	13.54	13.50	13.23
0.475		13.21	13.13	12.92
0.500	12.6	12.89	12.80	12.64
0.550	12.1	12.40	12.31	
0.600	11.6	11.99	11.89	
0.650	11.2	11.62	11.52	
0.700	10.8	11.27	11.17	
0.750	10.5	10.95	10.85	
0.800	10.2	10.64	10.55	

[a]Reference 3.

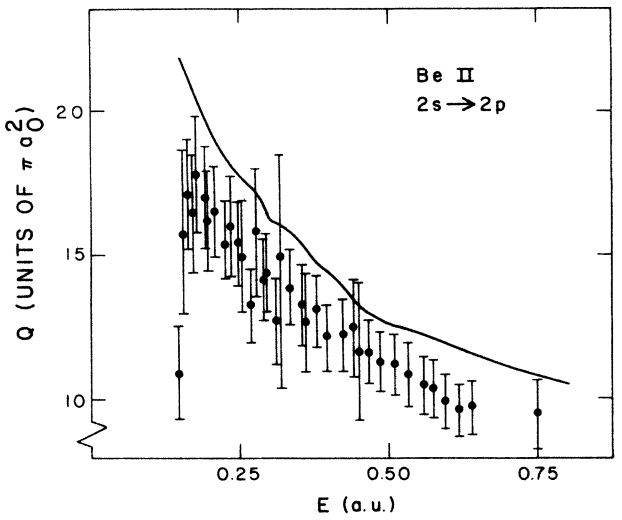

FIG. 1. Total inelastic cross section (Q) as a function of incident energy for the Be^+ $2s$-$2p$ transition. The measurements of Taylor, Phaneuf, and Dunn (Ref. 4) are shown as solid circles with error bars (representing total uncertainties at the 98% confidence level). The solid line represents CC9V cross sections for $E \leq 0.5$ a.u. and CC5V cross sections above 0.5 a.u. We do not show any other theoretical results on this diagram since the CC5 and PNP (Ref. 3) cross sections both lie very close to the solid curve.

correct cross sections are to be obtained for the $n=3$ states. Partial and total cross sections are tabulated separately for the $3s$, $3p$, and $3d$ levels in Tables X, XI, and XII. We have only tabulated what we believe are our best results. The CC9V results are used for $E \leq 0.5$ a.u., and the CC5V results are used for $E > 0.5$ a.u. As a result, there is a 20% discontinuity in the tabulated cross sections between 0.5 and 0.55 a.u. If values of the $n=3$ cross sections are needed for application, we would recommend that above $E=0.5$ a.u. the cross sections be scaled by the ratio of the CC9V and CC5V results at 0.5 a.u. Cross sections for the $n=3$ levels have been previously calculated.[3] While the total cross sections were calculated correctly, the partial cross sections for the individual magnetic sublevels of the $3p$ and $3d$ states were incorrectly calculated.

TABLE VIII. The partial cross sections (in units of πa_0^2) for excitation of the $2p$ ($M=0$) and $2p$ ($M=1$) levels (Q_0 and Q_1) as a function of the incident energy (in a.u.).

	CC5		CC5V		CC9V	
Energy	Q_0	Q_1	Q_0	Q_1	Q_0	Q_1
0.15	13.38	4.48	13.23	4.51	12.85	4.51
0.175	12.35	4.28	12.22	4.30	11.87	4.29
0.20	11.48	4.16	11.35	4.17	11.04	4.15
0.225	10.72	4.09	10.60	4.09	10.32	4.06
0.250	10.01	4.07	9.91	4.06	9.66	4.02
0.275	9.82	4.02	9.58	3.98	9.34	3.93
0.300	8.77	4.19	8.41	4.01	8.28	3.95
0.325	8.70	3.81	8.61	3.84	8.43	3.78
0.350	7.60	3.65	7.48	4.18	7.42	4.04
0.375	7.51	4.08	7.46	3.76	7.32	3.73
0.400	7.77	3.49	7.36	3.67	7.17	3.61
0.450	6.41	3.57	6.37	3.57	6.26	3.48
0.475	6.16	3.53	6.10	3.51	6.03	3.45
0.500	5.93	3.49	5.86	3.47	5.82	3.41
0.550	5.54	3.43	5.48	3.41		
0.600	5.21	3.39	5.16	3.36		
0.650	4.92	3.34	4.87	3.32		
0.700	4.66	3.30	4.61	3.28		
0.750	4.42	3.26	4.38	3.24		
0.800	4.21	3.22	4.16	3.19		

TABLE IX. Comparison of total excitation cross sections (in units of πa_0^2) for the $3s$, $3p$, and $3d$ levels of Be^+. Four different sets of results are shown.

Energy	PNP[a]	CC5	CC5V	CC9V
		$3s$		
0.450	0.59	0.596	0.585	0.505
0.475		0.590	0.579	0.490
0.500	0.57	0.581	0.570	0.471
		$3p$		
0.450	0.41	0.418	0.416	0.373
0.475		0.398	0.395	0.348
0.500	0.38	0.385	0.381	0.327
		$3d$		
0.450	0.54	0.572	0.537	0.459
0.475		0.643	0.610	0.518
0.500	0.66	0.691	0.658	0.556

[a]Reference 3.

VI. POLARIZATION OF THE FLUORESCENCE RADIATION

The percentage linear polarization for the $2p \rightarrow 2s$ decay is given by[23]

$$P = \frac{300(9\beta-2)(Q_0-Q_1)}{12Q_0+24Q_1+(9\beta-2)(Q_0-Q_1)}, \tag{11}$$

where Q_0 and Q_1 are the cross sections for excitation of the $M=0$ and $M=1$ levels and β is

TABLE X. The total cross section (in units of πa_0^2) for the excitation from the $2s$ level to the $3s$ level of Be^+. CC9V results are used for $E \leq 0.5$ a.u., above 0.5 a.u. CC5V results are tabulated.

Energy	Q
0.450	0.505
0.475	0.490
0.500	0.471
0.550	0.544
0.600	0.513
0.650	0.483
0.700	0.454
0.750	0.429
0.800	0.407

TABLE XI. Q_0 and Q_1 are, respectively, the cross sections (in units of πa_0^2) for excitation from the $2s$ level into the $3p$ ($M=0$) and $3p$ ($M=1$) levels of Be^+. The total cross section, $Q_{tot}=Q_0+2Q_1$ is also tabulated. CC9V results are used for $E \leq 0.5$ a.u., otherwise CC5V results are used.

Energy	Q_0	Q_1	Q_{tot}
0.450	0.260	0.057	0.373
0.475	0.241	0.054	0.348
0.500	0.227	0.050	0.327
0.550	0.252	0.050	0.352
0.600	0.236	0.042	0.320
0.650	0.219	0.035	0.289
0.700	0.203	0.030	0.263
0.750	0.189	0.026	0.241
0.800	0.176	0.023	0.222

$$\beta=(254+25f_{02}+30f_{12}+21f_{13}+70f_{23})/900 \quad (12)$$

for $^9Be^+$. The factors

$$f_{FF'}=[1+(2\pi\Delta\nu_{FF'}/A)^2]^{-1} \quad (13)$$

take into account precessional motions resulting from hyperfine splitting. Here, $\Delta\nu_{FF'}$ is the frequency separation between the hyperfine levels F and F' of the $2p_{3/2}$ state and A is the decay rate of this state (1.17×10^8 s^{-1}).

Previous calculations[1,3] of the linear polarization have given results considerably larger than the experimental data at low energies. However, it has been pointed out[6] that these previous calculations used an expression for the scattering amplitude which was not appropriate for *e*$^-$*-ion* collisions, and thus the polarization was incorrectly calculated. An additional error in Parpia, Norcross, and da Paixao[3] occurred in the determination of polarization at threshold. It was incorrectly stated that $Q_1/Q_0\rightarrow0$ at threshold. While this is true for atoms, it is not true for ions.

In order to compute the polarization from Q_0 and Q_1 it is necessary to have values for the hyperfine structure (HFS) splittings of the $2p_{3/2}$ levels. We determined the HFS splittings by using values for the electric quadrupole and magnetic dipole interaction constants from an accurate MBPT calculation.[24] The values are

$$A_{M1}=-1.49 \text{ MHz}$$

and

$$B_{E2}=2.26 \text{ MHz},$$

which yield a value for $\beta=0.4404$. If no HFS is assumed then $\beta=0.4444$. Other calculations of the hyperfine interaction constants[25,26] of the $2p_{3/2}$ level yield values of β almost the same, namely 0.431 (Ref. 25) and 0.433 (Ref. 26), respectively. The values we adopted for A_{M1} and B_{E2} are consistent with the available experimental data.[27]

TABLE XII. Q_0, Q_1, and Q_2, are, respectively, the cross sections (in units of πa_0^2) for excitation from the $2s$ level into the $3d$ ($M=0$, 1, and 2) levels. The total cross section Q_{tot} is $Q_0+2Q_1+2Q_2$. CC9V results were tabulated for $E \leq 0.5$ a.u., whereas CC5V results are used for $E > 0.5$ a.u.

Energy	Q_0	Q_1	Q_2	Q_{tot}
0.450	0.302	0.065	0.014	0.459
0.475	0.328	0.075	0.020	0.518
0.500	0.341	0.082	0.025	0.556
0.550	0.417	0.107	0.041	0.714
0.600	0.403	0.116	0.049	0.733
0.650	0.378	0.121	0.055	0.729
0.700	0.349	0.123	0.059	0.714
0.750	0.321	0.124	0.062	0.692
0.800	0.294	0.123	0.064	0.669

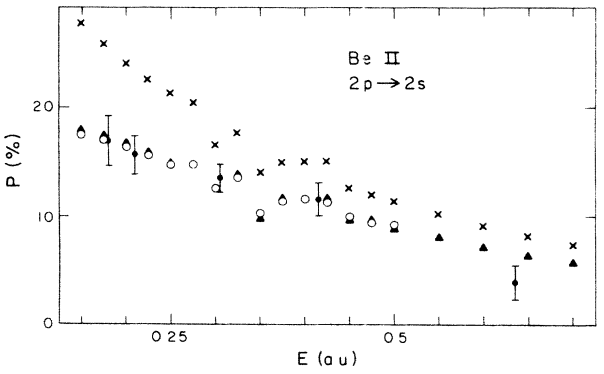

FIG. 2. Percentage linear polarization (P) of the Be^+ $2p\rightarrow2s$ fluorescence radiation, as a function of incident energy (in a.u.), following collisional excitation perpendicular to the scattering plane. The polarizations computed in the CC5V and CC9V approximations are shown as the solid triangles (▲) and open circles (○), respectively. When the CC5V and CC9V values of the polarization coincide, an open circle (○) is used. The incorrectly calculated values of the polarization [the Coulomb phase in Eq. (6) is omitted] using the CC5V K-matrix elements are depicted as crosses (×). The experimental data (Ref. 3) are shown as the solid circles with error bars (⧗).

We have used the values of Q_0 and Q_1 as given by the CC5V and CC9V calculations, along with a value of $\beta=0.4404$ to compute the polarization. A comparison of the theoretical and experimental polarization data is shown in Fig. 2. It is seen that the present calculations are in excellent agreement with experiment. We do not show results using values of Q_0 and Q_1 from the CC5 calculation since these are similar to the CC5V and CC9V calculations. We have also verified that we can reproduce the previous incorrectly calculated values of the polarization. Using values of Q_0 and Q_1 which are calculated incorrectly [the Coulomb phase in Eq. (6) is omitted], gives results which are similar to those calculated previously (see Fig. 2). These results remove one of the most disturbing differences between theory and experiment.

VII. SENSITIVITY TO VARIATIONS OF THE PSEUDOSTATES

It is now necessary to demonstrate that the results presented in the previous sections are not peculiar to the

TABLE XIII. Variation of Be atom binding energies (with respect to the Be^+ 2s threshold) as a function of the pseudostate excitation energy $\bar{\varepsilon}$.

State	Expt.	$\bar{\varepsilon}$ 0.605[a]	0.700	0.800	0.900	1.000	1.100
$2s^2\,{}^1S^e$	−0.342 60	−0.342 37	−0.342 47	−0.342 51	−0.342 52	−0.342 51	−0.342 50
$2s3s\,{}^1S^e$	−0.093 47	−0.093 48	−0.093 49	−0.093 49	−0.093 48	−0.093 48	−0.093 48
$2s2p\,{}^1P^o$	−0.148 66	−0.147 71	−0.148 04	−0.148 16	−0.148 21	−0.148 22	−0.148 22
$2s3p\,{}^1P^o$	−0.068 37	−0.068 13	−0.068 18	−0.068 21	−0.068 22	−0.068 23	−0.068 23
$2s2p\,{}^3P^o$	−0.242 45	−0.242 41	−0.242 45	−0.242 47	−0.242 48	−0.242 48	−0.242 48
$2p^2\,{}^3P^e$	−0.070 61	−0.070 00	−0.070 37	−0.070 43	−0.070 43	−0.070 42	−0.070 38

[a]The $\overline{4s}$ state was located at an energy 0.690 83 a.u. above the Be^+ 2s ground state

specific choice of the degenerate pseudostates. The pseudostates can be varied systematically by changing the exponential parameters (α_l) and thus changing the excitation threshold of the pseudostates. Pseudostates with excitation thresholds of 0.7, 0.8, 0.9, 1.0, and 1.1 a.u. were generated by this method. Due to lack of variational flexibility in the $l=0$ and 1 pseudostates, it was not possible to generate $l=0$ and 1 pseudostates with an excitation energy of 0.6 a.u. Instead, $l=1$, 2, and 3 pseudostates at an excitation energy of 0.605 a.u. were used in conjunction with a $\overline{4s}$ state located at 0.690 83 a.u. above the ground state.

The variation of some typical bound state binding energies as a function of pseudostate energy is shown in Table XIII. In general the quality of the results is almost independent of the pseudostate energy in the range $\bar{\varepsilon}=0.7\rightarrow 1.1$ a.u. There is some degradation in the quality of the results for the $\bar{\varepsilon}=0.605$ basis. This is to be expected, since the $\bar{\varepsilon}=0.605$ pseudostates would have a large overlap with diffuse $n=4$ Rydberg states. It has often been remarked[28] that diffuse Rydberg-type states do not lead to as large a reduction in the binding energy in variational calculations as more radially compact functions.

The variation of the most important partial cross sections (i.e., the largest) with pseudo-state energy is shown in Table XIV. In all cases, the variation of the partial cross sections across the entire range of pseudostate energies is less than 1%. These results demonstrate that the small differences reported between the CC5V and CC9V cross sections is not a feature peculiar to the particular choice (i.e., $\bar{\varepsilon}=0.9$) used for the degenerate $n=4$ pseudostates.

VIII. CONCLUSION

We have completed a series of calculations of increasing sophistication in an attempt to unravel the reasons for the discrepancies between theoretical and experimental excitation cross sections for the resonance transition in Be^+. We have used subsidiary data, namely Be atom binding energies and resonance positions, to provide a test of the quality of our $Be^+ + e^-$ model wave functions. In almost every instance it is found that as the size of calculation increases, the agreement between theory and experiment for this subsidiary data is improved. The agreement between our most sophisticated calculation (CC9V) and most experimental data is very good. However, there is almost no change ($\lesssim 2\%$) in the theoretical cross section for 2s-2p excitation as the size of the calculation is increased; the theoretical cross sections remain larger than experiment by 18% (independent of energy). This is particularly disturbing since the distinctions between theory and experiment remain as glaring as ever even though our cross section calculations appear to have converged with respect to increasing number of channels.

TABLE XIV. Variation of the $L=1$, 3, and 4 partial cross sections of the CC9V calculation for the 2s-2p transition (in units of πa_0^2) as a function of the pseudostate excitation energy $\bar{\varepsilon}$. Values are presented for two different incident energies.

L	CC5V	$\bar{\varepsilon}$ 0.605[a]	0.700	0.800	0.900	1.0	1.10
				$E=0.15$ a.u.			
1	2.897	2.858	2.847	2.850	2.854	2.858	2.863
3	10.918	10.733	10.720	10.728	10.745	10.760	10.775
4	5.260	5.220	5.215	5.216	5.218	5.221	5.221
				$E=0.25$ a.u.			
1	1.809	1.767	1.757	1.759	1.763	1.769	1.774
3	5.130	5.007	4.992	4.997	5.006	5.018	5.028
4	4.935	4.878	4.873	4.878	4.882	4.885	4.889

[a]The $\overline{4s}$ state was located at an energy of 0.690 83 a.u. above the Be^+ 2s ground state.

ACKNOWLEDGMENTS

This work has been supported by the United States Department of Energy (Division of Chemical Sciences, Office of Basic Energy Sciences, Office of Energy Research). We are grateful to G. Dunn for a tabulation of his group's experimental data, and to D. R. Beck and W. R. Johnson for providing us with the results of refined hyperfine-structure calculations prior to publication. The initial assistance of F. A. Parpia has been quite valuable. The calculations performed in this work were done with the Control Data Corporation Cyber-205 computer at National Bureau of Standards (NBS), Gaithersburg, MD and the Digital Equipment Corporation VAX-8600 computer at Joint Institute of Laboratory Astrophysics (JILA), Boulder, CO.

---

*Quantum Physics Division, National Bureau of Standards, Boulder, CO 80309-0440.

[1]M. A. Hayes, D. W. Norcross, J. B. Mann, and W. D. Robb, J. Phys. **11**, L429 (1977).

[2]R. J. W. Henry, W.-L. van Wyngaarden, and J. J. Matese, Phys. Rev. A **17**, 798 (1978).

[3]F. A. Parpia, D. W. Norcross, and F. J. da Paixao, Phys. Rev. A **34**, 4777 (1986); **36**, 1510 (1987).

[4]P. O. Taylor, R. A. Phaneuf, and G. H. Dunn, Phys. Rev. A **22**, 435 (1980).

[5]R. A. Falk and G. H. Dunn, Phys. Rev. A **27**, 754 (1983).

[6]J. Mitroy, Phys. Rev. A **37**, 649 (1988).

[7]H. A. Saraph, J. Phys. B **3**, 952 (1970).

[8]This program is unpublished. Recent references are P. G. Burke and W. Eissner, in *Atoms in Astrophysics*, edited by P. G. Burke, W. B. Eissner, D. G. Humnaer, and I. C. Percival (Plenum, New York, 1983); H. Nussbaumer and P. J. Storey, *ibid.*

[9]M. A. Crees, M. J. Seaton, and P. M. H. Wilson, Comput. Phys. Commun. **15**, 23 (1978).

[10]M. J. Seaton, J. Phys. B **7**, 1817 (1974).

[11]A. W. Weiss, Astrophys. J. **138**, 1262 (1963).

[12]C. Froese Fischer, Comp. Phys. Commun. **14**, 145 (1978).

[13]S. Bashkin and J. O. Stoner, *Atomic Energy Levels and Grotrian Diagrams* (North-Holland, Amsterdam, 1975), Vol. 1.

[14]D. W. Norcross and M. J. Seaton, J. Phys. B **9**, 2983 (1976).

[15]P. Sitz, J. Chem. Phys. **55**, 1481 (1971).

[16]R. Moccia and P. Spizzo, J. Phys. B **18**, 3537 (1985).

[17]A. W. Weiss, Phys. Rev. A **6**, 1261 (1972).

[18]C. W. Clark, J. B. Fassett, T. B. Lucatorto, L. J. Moore, and W. W. Smith, J. Opt. Soc. Am. B **2**, 891 (1985).

[19]G. Mehlman-Balloffet and J. M. Esteva, Astrophys. J. **157**, 945 (1969).

[20]L. Johansson, Ark. Fys. Semin. Trondheim **23**, 119 (1962).

[21]F. Paschen and P. G. Kruger, Ann. Phys. (Leipzig) **8**, 1005 (1931).

[22]C. Bottcher, J. Phys. B **3**, 1201 (1970).

[23]D. R. Flower and M. J. Seaton, Proc. Phys. Soc. London **91**, 59 (1967).

[24]W. R. Johnson (private communication).

[25]D. R. Beck (private communication).

[26]S. Garpman, I. Lindgren, J. Lindgren, and J. Morrison, Z. Phys. A **276**, 167 (1976).

[27]O. Paulsen, T. Andersen, and N. J. Skoube, J. Phys. B **9**, 1393 (1975).

[28]A. W. Weiss, Adv. At. Mol. Phys. **9**, 1 (1973).